The Astrophysical Journal, 644:587–591, 2006 June 10

CATASTROPHE OF CORONAL FLUX ROPE IN UNSHEARED AND SHEARED BIPOLAR MAGNETIC FIELDS

Y. Chen, X. H. Chen, and Y. Q. Hu
CAS Key Laboratory of Basic Plasma Physics, School of Earth and Space Sciences, University of Science and Technology of China, Hefei, Anhui 230026, China; yaochen@ustc.edu.cn
Received 2005 December 11; accepted 2006 February 15

ABSTRACT

This article investigates the catastrophic behavior of a preexisting coronal magnetic flux rope embedded in a dipolar or partially open bipolar background field, which is either unsheared or sheared with a given footpoint displacement of magnetic field lines. It is found that in the unsheared background field the catastrophic energy threshold decreases slightly with increasing extent of opening of the background field and increasing annular flux or decreasing axial flux of the flux rope, varying in the range between 1.08 and 1.1 times the magnetic energy of the corresponding fully open field. As the background field is sheared, on the other hand, catastrophe may be triggered by shear provided that the presheared magnetic energy of the system is high enough. The catastrophic energy threshold is almost invariant but then increases monotonically with the increase of the presheared magnetic energy of the system, and it is bounded above by the energy of the corresponding flux rope system associated with an unsheared background field.

Subject headings: Sun: corona — Sun: coronal mass ejections (CMEs)

1. INTRODUCTION

The catastrophic model of a coronal magnetic flux rope is one of the promising scenarios for solar eruptions such as coronal mass ejections (CMEs), flares, and prominence eruptions (reviewed recently by Lin et al. 2003; Hu 2005). With this scenario, the magnetic energy that has been stored in the corona is suddenly released as a result of the destabilization of the global magnetic field topology; the flux rope is then expelled outward by the unbalanced Lorentz force with a velocity comparable to the local Alfvén speed. Recently, Hu and his coauthors carried out numerical calculations studying the catastrophe of the coronal flux rope embedded in different background fields. They found an occurrence of a catastrophe in either a dipolar or a partially open bipolar field (Hu et al. 2003; Li & Hu 2003), or a quadrupolar field (Zhang et al. 2005), and in other multipolar fields as well (Peng & Hu 2005; Ding & Hu 2006). The total magnetic energy at the catastrophic point representing the maximum energy that the system can contain is defined as the catastrophic energy threshold. When the energy of the system reaches or exceeds the threshold, the catastrophe takes place causing the eruption of the flux rope. Among these studies, Li & Hu (2003) argued that the catastrophic energy threshold is almost constant and exceeds about 8% of the corresponding fully open bipolar field energy. However, this conclusion is based on only four solutions corresponding to a dipolar field and a partially open bipolar field for flux ropes with different magnetic fluxes. Section 3 of this paper further explores the impact of the background field and flux rope parameters on the catastrophic energy threshold by extending the study to a larger parameter space.

Most of the present catastrophic models presumed that the background field is potential without shear motion. However, it is widely believed that the shear motion on the photosphere is critical to the energy storage process in the corona and may serve as one of the triggering mechanisms to solar eruptions (e.g., Mikić & Linker 1994). For instance, Hu & Jiang (2001) found that in the Cartesian geometry the footpoint shear motion of the background magnetic field is capable of triggering the flux rope catastrophe. In this paper we construct the coronal flux rope model with sheared background field in spherical coordinates to seek answers to the following questions: (1) Can the shear motion on the photosphere trigger the flux rope catastrophe in spherical coordinates? (2) If yes, how does the shear affect the catastrophic energy threshold? There are two methods of shearing a magnetic field in the literature: one is to specify directly the pattern and amplitude of the sheared component of the magnetic field on the photosphere (e.g., Flyer et al. 2004), and the other is to specify the footpoint displacement of the field lines (e.g., Mikić & Linker 1994; Antiochos et al. 1999). The latter is believed to be more appropriate in modeling solar magnetic fields (Klimchuk & Sturrock 1989). Recently, Hu & Wang (2005) designed a method to implement a given footpoint displacement accurately in the numerical sense. In § 4 of this paper we adopt this method to shear the background field in order to examine the response of the magnetic flux rope system and to make a comparison with the case without shear. Section 5 provides a summary of this article with a brief discussion.

2. REPRESENTATION OF THE CORONAL FLUX ROPE SYSTEM

For the axisymmetric magnetohydrodynamic (MHD) system, one can introduce the magnetic flux function $\psi(t, r, \theta)$ to express the magnetic field $\boldsymbol{B}(B_r, B_\theta, B_\varphi)$ as

$$\boldsymbol{B} = \nabla \times \left(\frac{\psi}{r \sin \theta} \hat{\boldsymbol{\varphi}} \right) + B_\varphi \hat{\boldsymbol{\varphi}}. \tag{1}$$

The derived ideal MHD equations can be found in Hu (2004) and are not repeated here. Assume that the initial background atmosphere is polytropic in static equilibrium with temperature and density given by (e.g., Low 1984)

$$T(r) = T_0 r^{-1}, \quad \rho(r) = \rho_0 r^{-1/(\gamma-1)}, \tag{2}$$

where $\gamma = 1.21$ is the polytropic index, r represents the heliocentric distance in units of solar radius $R_\odot$, and T_0 and ρ_0 are the base temperature and density, taken to be 2 MK and 1.67×10^{-13} kg m^{-3}, respectively. It can be seen that from the coronal base to 10 $R_\odot$, the temperature decreases by a factor of 10 and the density decreases by 4–5 orders of magnitude. This is in general agreement with the solar wind model (see, e.g., Chen &

Hu 2001; Hu et al. 2003). In the calculation to be presented, the density and temperature are fixed to their initial values so as to achieve strictly force-free field solutions. (This method is called the "relaxation method," first given by Hu 2004.) In previous models the initial corona is usually assumed to be isothermal. It is demonstrated by tentative calculations that the background atmosphere is important to the velocity profile of the erupting flux rope after catastrophe, but it has little bearing on the catastrophic behavior and energy threshold. The purpose of using a polytropic atmosphere here is for future study on the CME propagation in terms of the same model. The initial background magnetic field is either a dipolar or a partially open bipolar field. For the dipolar field, the flux function is given by $\psi(r, \theta) = \sin^2\theta/r$ (all magnetic fluxes in this article are in units of $\psi_0 = 5.69 \times 10^{14}$ Wb, which is the total magnetic flux of the background magnetic field), and the associated magnetic field strength at the base along the equator is $B_0 = \psi_0/R_\odot^2 \approx 11.7$ G. Starting from the dipolar field, the partially open one with an equatorial current sheet extending to infinity can be obtained through specifying the minimum magnetic flux function along the equator (see Hu & Wang 2005). The obtained magnetic topologies have the same flux distribution at the base as the dipolar field. To characterize the extent of opening of these fields, we define a parameter ϵ as the ratio of the open to the total magnetic flux at the base: $\epsilon = 0$ corresponds to the dipolar field and $\epsilon = 1$ to the fully open one. In § 3 we examine the effect of the background field on the flux rope catastrophe with ϵ varying from 0 to 0.8. After the background field is established, we let a flux rope emerge from the base into the closed magnetic arcade in a short time τ_E within a specified range of latitude bounded by $\lambda \equiv \theta - \pi/2 = \pm\lambda_E$ (Hu et al. 2003), and

$$\lambda_E(t) = 2\lambda_w \left[\frac{t}{\tau_E}\left(1 - \frac{t}{\tau_E}\right)\right]^{1/2}, \tag{3}$$

where λ_w denotes the maximum half-width of the emerging flux rope. The base parameters in the process of flux rope emergence are taken as follows in computational units:

$$\psi(t, 1, \theta) = \psi(0, 1, \theta) + \psi_E(t, \theta), \tag{4}$$

$$\psi_E(t, \theta) = \frac{C_E\left(\lambda_E^2 - \lambda^2\right)}{\lambda_w^2}, \tag{5}$$

$$B_\varphi(t, 1, \theta) = \frac{B_{\varphi 0}\left(\lambda_E^2 - \lambda^2\right)^{1/2}}{\lambda_w}, \tag{6}$$

$$v_r(t, 1, \theta) = \frac{2\lambda_w}{\tau_E}, \tag{7}$$

$$v_\theta(t, 1, \theta) = v_\varphi(t, 1, \theta) = 0, \tag{8}$$

$$T(t, 1, \theta) = \rho(t, 1, \theta) = 1, \tag{9}$$

where the constants C_E and $B_{\varphi 0}$ are used to determine the magnetic properties of the emerging flux rope and thus the obtained whole system. The computational units for the magnetic fluxes, magnetic field strength, velocity, plasma temperature, and density are ψ_0, B_0, v_{A0} (where $v_{A0} = 2571$ km s^{-1} is the Alfvén speed at the base), T_0, and ρ_0, respectively. After $t > \tau_E$, the base boundary conditions return to the original ones. The associated parameters $\tau_A = R_\odot/v_{A0}$ and $\lambda_E = 0.087$ rad (i.e., 5°). The resulting levitating flux rope reaches an equilibrium state in a sufficiently long time of relaxation (e.g., $500\tau_A$). The annular and axial fluxes of the flux rope turn out to be 0.3 and 0.15, respectively. Starting from this equilibrium state, we can adjust the two fluxes step by step so as to obtain other equilibrium solutions, and each of them is characterized by a specific set of the two rope fluxes.

TABLE 1
THE MAGNETIC ENERGY E_b OF THE BACKGROUND MAGNETIC FIELD VERSUS THE OPEN LEVEL ϵ

ϵ	E_b
0.0	0.3334
0.1	0.3335
0.2	0.3350
0.3	0.3389
0.4	0.3465
0.5	0.3592
0.6	0.3782
0.7	0.4052
0.8	0.4418
1.0	0.5539

The background field of the flux rope system is sheared in the way given by Hu & Wang (2005). The associated azimuthal displacement of the shear motion (defined as half of the relative displacement between the two footpoints of one single magnetic field line) is given by

$$\delta\varphi(\theta) = \varphi_m \cos\left[\frac{\pi(2\theta - \theta_1 - \theta_2)}{2(\theta_2 - \theta_1)}\right], \tag{10}$$

where (θ_1, θ_2) determines the shear region, taken to be (50.°8, 71.°6), which corresponds to a range of (0.6, 0.9) for the magnetic flux function at the base, and φ_m represents the maximum displacement (called "shear amplitude" hereafter) located at $\theta_m = (\theta_1 + \theta_2)/2$. For a given shear amplitude φ_m, one can get the associated coronal flux rope equilibrium. The total magnetic energy is given by (Hu & Wang 2005)

$$E = \frac{1}{2}\int_1^{30} dr \int_0^{\pi/2} B^2 r^2 \sin\theta\, d\theta + \frac{30^3}{2}\int_0^{\pi/2} \left(B_r^2 - B_\theta^2\right)_{r=30} \sin\theta\, d\theta, \tag{11}$$

with E to be normalized by $4\pi B_0^2 R_\odot^3/\mu_0$ and $B = (B_r^2 + B_\theta^2 + B_\varphi^2)^{1/2}$ in units of B_0. With the use of equation (11), we calculate the energy of the initial background in the absence of shear and flux rope, denoted by E_b and listed in Table 1 as a function of ϵ. We can see that E_b increases monotonically with increasing ϵ as expected.

3. FLUX ROPE CATASTROPHE ASSOCIATED WITH UNSHEARED BACKGROUND FIELDS

In this section we present numerical results associated with unsheared background bipolar fields ($\epsilon \leq 0.8$). We obtain the equilibrium solutions of the coronal flux rope system with the annular flux of the rope $\Phi_p = 0.3$ for each background field. The catastrophic point of the system can be located through adjusting the axial flux of the rope Φ_φ gradually in an appropriate range. As expected from previous similar studies, the flux rope is always attached to the photosphere in equilibrium when Φ_φ is less than a critical value $\Phi_{\varphi c}$; once $\Phi_\varphi > \Phi_{\varphi c}$, a catastrophe takes place resulting in the fast eruption of the flux rope. Thus, we can obtain all the critical axial flux and the associated energy

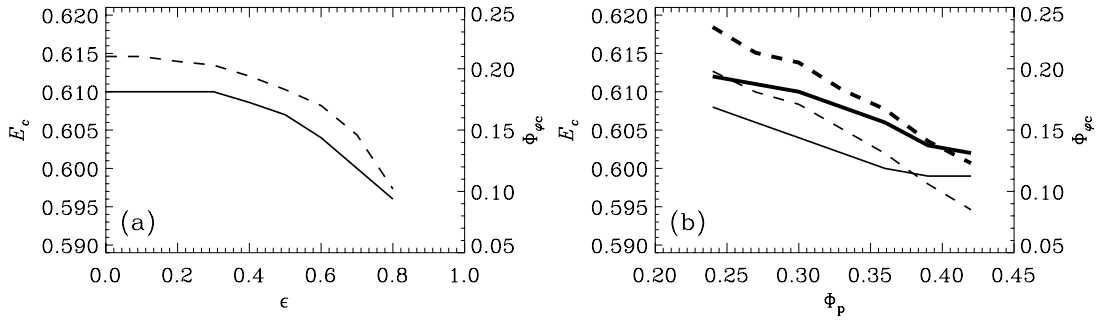

FIG. 1.—(*a*) Variations of the catastrophic energy threshold E_c (*solid line*) for the flux rope with annular flux $\Phi_p = 0.3$ and the associated axial flux at the catastrophic point $\Phi_{\varphi c}$ (*dashed line*) with the open level of the background magnetic field ϵ. (*b*) Quantities E_c (*solid lines*) and $\Phi_{\varphi c}$ (*dashed lines*) for the flux rope with different annular flux Φ_p in the bipolar background field with $\epsilon = 0.4$ (*thick lines*) and 0.6 (*thin lines*).

threshold E_c for the flux rope with $\Phi_p = 0.3$ in the bipolar fields considered. The results are plotted in Figure 1*a* with dashed ($\Phi_{\varphi c}$) and solid lines (E_c). For the dipolar field ($\epsilon = 0$) we have $E_c = 0.610$, and for the partially open bipolar field with $\epsilon = 0.8$, we have $E_c = 0.596$. The energy threshold is almost independent of ϵ for $\epsilon \leq 0.4$ but decreases monotonically with increasing ϵ for $\epsilon > 0.4$. The energy threshold E_c varies between 1.08 and 1.1 times the energy of the corresponding fully open bipolar field. In addition, the critical axial flux $\Phi_{\varphi c}$ at the catastrophic point also decreases monotonically with increasing ϵ, as expected.

In the above calculations the annular flux of the rope is fixed to be $\Phi_p = 0.3$. To further examine the effect of Φ_p on the catastrophic energy threshold, we calculate E_c and $\Phi_{\varphi c}$ as a function of Φ_p for two different background fields with $\epsilon = 0.4$ and 0.6, respectively. The results are shown in Figure 1*b* with solid (E_c) and dashed lines ($\Phi_{\varphi c}$). The left (right) ordinate gives the scales of the energy (the critical axial flux), and the thick (thin) curves denote the solutions associated with $\epsilon = 0.4$ (0.6). It can be seen from Figure 1*b* that the energy threshold is smaller for a higher open level of the background field, agreeing with the results shown in Figure 1*a*, and decreases monotonically with increasing Φ_p. Note that in the study by Li & Hu (2003), only two background fields were considered, the dipolar one and the partially open one with $\epsilon \approx 0.6$, and the annular flux of the rope lies between 0.4 and 0.5. From the numerical results obtained in these special cases, they argued that the catastrophic energy threshold is roughly constant, about 1.08 times the corresponding fully open field energy. The cases treated by them are situated at the lower right corner of Figure 1*b*, and their results are therefore consistent with ours. Moreover, the critical axial flux $\Phi_{\varphi c}$ at the catastrophic point decreases monotonically with increasing Φ_p. As a matter of fact, Figure 1*b* depicts the loci of the catastrophic points in the Φ_p-Φ_φ plane, so the abscissa represents in essence the critical annular flux, Φ_{pc}, at the catastrophic point. Since $\Phi_{\varphi c}$ decreases monotonically with increasing Φ_{pc} along these loci, it becomes obvious that the energy threshold increases with decreasing Φ_φ. In summary, we conclude that the catastrophic energy threshold varies in a range of 1.08–1.1 times the magnetic energy of the fully open field depending on the open level of the background field and the flux rope properties.

4. FLUX ROPE CATASTROPHE IN SHEARED BACKGROUND FIELDS

Now we consider the cases with sheared background field. Only the solutions for the partially open bipolar field with $\epsilon = 0.4$ are discussed. For background fields with other values of ϵ, there exist dependences of the flux rope catastrophe on the shear of the background field similar to those to be presented below. In the following we select two groups of flux ropes with $\Phi_p = 0.3$ and 0.24 for the purpose of parameter study. The corresponding catastrophic energy threshold and critical axial flux (E_c, $\Phi_{\varphi c}$) are (0.608, 0.194) and (0.612, 0.233), respectively, in the unsheared background as seen from Figure 1*b*. The two energy thresholds are shown as thin horizontal lines in Figure 2. In each group, the flux rope differs in Φ_φ. For each given set of (Φ_p, Φ_φ), an equilibrium is obtained through numerical simulations. The magnetic energy of the equilibrium (called the "presheared magnetic energy" in the following text) increases monotonically with increasing Φ_φ, as shown by the dotted lines in Figures 2*a* ($\Phi_p = 0.3$) and 2*b* ($\Phi_p = 0.24$). Starting from the obtained

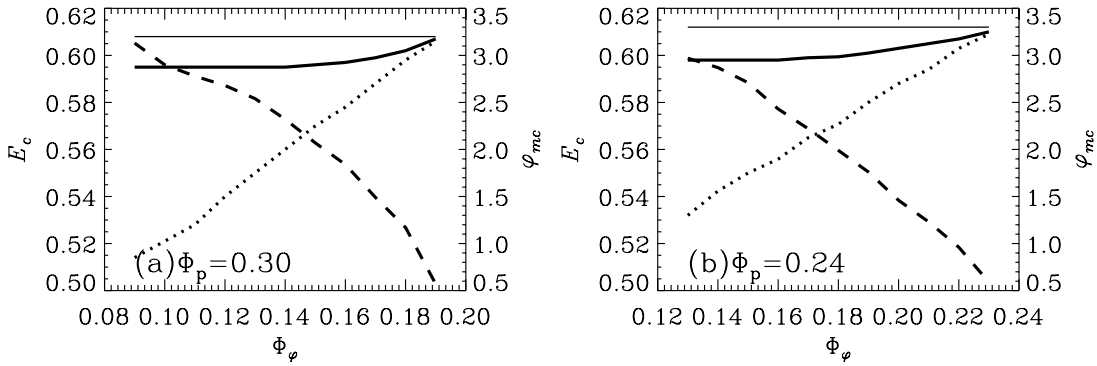

FIG. 2.—Presheared energy of the coronal flux rope system (*dotted lines*) in the partially open bipolar field with $\epsilon = 0.4$ and the annular flux of the rope for (*a*) $\Phi_p = 0.3$ (*b*) $\Phi_p = 0.24$, the energy threshold of the system catastrophe triggered by the photospheric shear motion E_c (*thick solid lines*), and the corresponding critical shear amplitude φ_{mc} (*dashed lines*) with different axial flux of the rope Φ_φ. The thin solid horizontal lines represent the catastrophic energy threshold for the flux rope system with the same annular flux in the corresponding unsheared background.

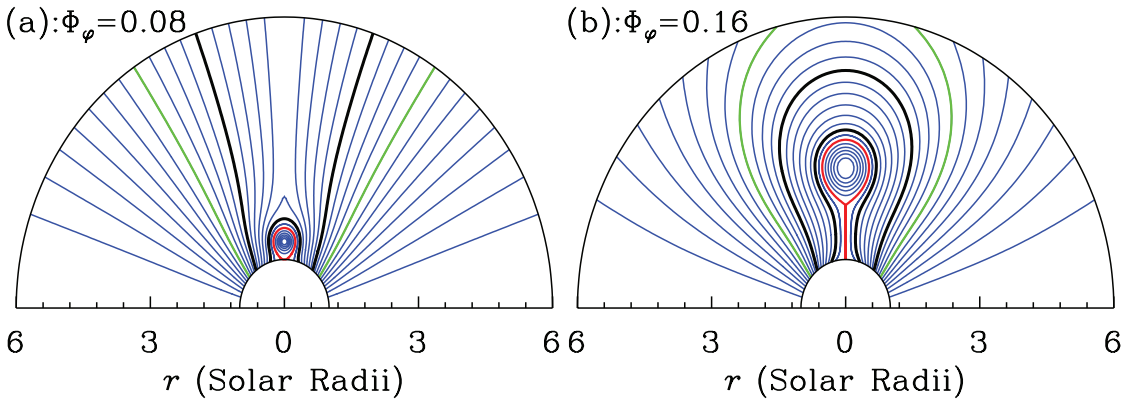

FIG. 3.—Magnetic topology (ψ, *contours*, uniformly spaced 0.05 apart) of two cases with flux rope parameters (*a*) $\Phi_p = 0.3$, $\Phi_\varphi = 0.08$ and (*b*) $\Phi_p = 0.3$, $\Phi_\varphi = 0.16$. Please see the text for details.

equilibria, we shear the background field to achieve a footpoint displacement given by equation (10). To keep the system evolving quasi-statically, we increase the shear amplitude slowly and linearly with time until it reaches the prespecified magnitude at $t = 300\tau_A$ and then keep the shear amplitude invariant. The time-dependent simulation continues until the system reaches equilibrium. The magnetic energy of the system thus obtained increases monotonically with the increase of the shear amplitude φ_m. When φ_m exceeds a certain critical value, the catastrophe sets in. For instance, the flux rope with $(\Phi_p, \Phi_\varphi) = (0.3, 0.16)$ remains attached to the photosphere in equilibrium for $\varphi_m = 1.83$ but erupts upward for $\varphi_m = 1.84$, indicating an occurrence of catastrophe. Then we obtain the critical shear amplitude at the catastrophic point $\varphi_{mc} = 1.84$ and the associated energy threshold $E_c = 0.597$. We plot the profiles of φ_{mc} (*dashed lines*) and E_c (*thick solid lines*) versus the axial flux of the rope Φ_φ for $\Phi_p = 0.3$ and 0.24 in Figures 2*a* and 2*b*, respectively. The critical shear amplitude φ_{mc} decreases monotonically with increasing Φ_φ for the two cases as expected. The energy threshold E_c is bounded above by that in the unsheared background field case (*thin horizontal line*). It keeps constant for $\Phi_\varphi < 0.14$ in the $\Phi_p = 0.3$ case (Fig. 2*a*, $E_c = 0.595$) and for $\Phi_\varphi < 0.18$ in the $\Phi_p = 0.24$ case (Fig. 2*b*, $E_c = 0.598$) and increases with increasing Φ_φ hereafter. Nevertheless, the variation of the catastrophic energy threshold remains relatively small, less than 2.3% for the present cases.

Incidentally, when the axial flux of the rope Φ_φ is too small, the catastrophe does not appear even if the shear is strong enough to open the magnetic field in the shear region. The magnetic topology (ψ, *contours*, uniformly spaced 0.05 apart) of such an example is shown in Figure 3*a* with parameters $\Phi_p = 0.3$, $\Phi_\varphi = 0.08$, and $\varphi_m \approx 7$. For comparison, the magnetic topology for the system with an erupting flux rope, $6\tau_A$ after the catastrophe, is shown in Figure 3*b* with parameters $\Phi_p = 0.3$, $\Phi_\varphi = 0.16$, and $\varphi_m \approx 1.84$. The red lines represent the boundary of the flux rope and the vertical current sheet below formed by the rope eruption, the thick black lines depict the inner and outer boundaries of the sheared field, and the green lines delineate the border between the closed and open field region of the background. In Figure 3*a*, the rope remains to be attached to the photosphere, although the outermost part of the sheared field has been opened. This means that with the shear displacement defined by equation (10), a catastrophe can occur only if the presheared magnetic energy of the flux rope system is above a certain critical value. From the energy analysis, it is inferred that this critical energy lies between 0.50 and 0.515 for $\Phi_p = 0.3$ and between 0.52 and 0.53 for $\Phi_p = 0.24$. Of course, such inference applies only to the specific shear pattern defined in equation (10).

5. CONCLUSIONS AND DISCUSSION

The catastrophic behaviors of a coronal flux rope embedded in unsheared and sheared bipolar background fields were investigated. It is found that the catastrophic energy threshold of the flux rope system depends weakly on the open level of the background bipolar field and the flux rope parameters. The energy threshold varies in a range of 1.08–1.1 times the magnetic energy of the corresponding fully open field. Applying photospheric shear motion with specified footpoint displacement, we have constructed the catastrophic flux rope model with sheared bipolar background fields in spherical geometry. The main conclusions are summarized below: (1) A catastrophe of the flux rope system may be triggered by shearing the background field when the presheared magnetic energy of the flux rope system is high enough. (2) The associated catastrophic energy threshold is bounded above by that in the unsheared case, and it is almost invariant but then increases monotonically with the increase of the presheared magnetic energy of the flux rope system. (3) In various bipolar background fields, either unsheared or sheared, the catastrophic energy threshold changes with the open level of the background field and the flux rope parameters, in a relatively small range, approximately from 1.08 to 1.1 times the corresponding open field energy.

Although the above conclusion regarding the value and range of the catastrophic energy threshold is not based on an exhaustive parameter study, it seems to be a rather general result for the flux rope system with a bipolar ambient field. The catastrophic energy threshold always exceeds the energy of the corresponding fully open field by a certain value. The excess energy will be released in a short timescale to open the ambient field and accelerate the erupting flux rope after catastrophe. This is a general point of the current work, as well as previous studies in this series (Hu 2005), but it is different from that presented by Lin et al. (1998). They showed (also in axisymmetric spherical coordinates) that the maximum magnetic energy of the flux rope system is below that of the corresponding open field. Note that for mathematical tractability, Lin et al. assumed the flux rope radius to be much smaller than the surrounding poloidal-flux bubble (classified as thin-rope model by Hu 2005), while in our studies there is no such simplification (i.e., thick-rope

model). This may account for the contrasting difference between the results regarding the energy threshold obtained by the two scenarios. Further study to clarify this point is necessary to fill in the gap between the two models, which can be taken as one of our future tasks.

Considering that the catastrophe can take place for the flux rope system without any shear motion, while pure photospheric shear motion exerting on simple arcades (e.g., a bipolar or quadrupolar field without flux rope embedded) can at most open the arcades without catastrophe (Mikić & Linker 1994; Hu 2004), it is easy to see that for the flux rope catastrophe to be triggered by photospheric shear motions, the presheared flux rope system has to be close enough to the catastrophic point. The energy of the presheared system already exceeds the open field energy according to our study. The system energy increases when the photospheric footpoints are sheared. Once the catastrophe sets in, the free energy deposited by the original flux rope and the shear of the ambient arcade is released to open the overlying arcade and accelerate the erupting flux rope. Mikić & Linker (1994) sheared a simple arcade field without a flux rope embedded; therefore, the energy of the system never exceeds the fully open field energy, which agrees with the Aly conjecture (Aly 1984). Thus, nonideal MHD process such as magnetic reconnection must be invoked to form and accelerate CMEs in the model of Mikić & Linker.

The catastrophe of the magnetic system provides a straightforward mechanism for the sudden release of magnetic energy in CMEs. This process is an ideal MHD phenomenon in nature, accompanied by a sudden magnetic energy release and the formation of a vertical current sheet. The latter provides an appropriate condition for fast magnetic reconnection, which reduces the constraining force yielded by the background field on the flux rope (see, e.g., Lin & Forbes 2000), and further transforms part of the magnetic energy into thermal and kinetic energies of the coronal plasma. In addition, the plasma and magnetic field carried on by CMEs will interact with the background solar wind. Since the aim of this article is to find the metastable state of the flux rope system and explore the physics near the catastrophic point, effects of magnetic reconnection and solar wind have not been taken into account. These effects will be incorporated into our future studies of catastrophic models with implications for CMEs in order to carry out detailed comparisons with observational data currently available.

This work was supported by grants NNSFC 40404013, 40274049, and 10233050 and the Key Program of the Chinese Academy of Science (KZCX3-SW-144). Y. Chen thanks J. Lin, G. Q. Li, J. Y. Ding, and Sh. J. Sun for helpful discussions.

REFERENCES

Aly, J. J. 1984, ApJ, 283, 349
Antiochos, S. K., DeVore, C. R., & Klimchuk, J. A. 1999, ApJ, 510, 485
Chen, Y., & Hu, Y. Q. 2001, Sol. Phys., 199, 371
Ding, J. Y., & Hu, Y. Q. 2006, Sol. Phys., 233, 45
Flyer, N., Fornberg, B., Thomas, S., & Low, B. C. 2004, ApJ, 606, 1210
Hu, Y. Q. 2004, ApJ, 607, 1032
———. 2005, in IAU Symp. 226, Coronal and Stellar Mass Ejections, ed. K. Dere, J. Wang, & Y. Yan (Cambridge: Cambridge Univ. Press), 263
Hu, Y. Q., Habbal, S. R., Chen, Y., & Li, X. 2003, J. Geophys. Res., 108, 1377
Hu, Y. Q., & Jiang, Y. W. 2001, Sol. Phys., 203, 309
Hu, Y. Q., Li, G. Q., & Xing, X. Y. 2003, J. Geophys. Res., 108 (A2), 1072
Hu, Y. Q., & Wang, Zh. 2005, ApJ, 623, 551
Klimchuk, J. A., & Sturrock, P. A. 1989, ApJ, 345, 1034
Li, G. Q., & Hu, Y. Q. 2003, Chinese J. Astron. Astrophys., 3, 555
Lin, J., & Forbes, T. G. 2000, J. Geophys. Res., 105 (A2), 2375
Lin, J., Forbes, T. G., Isenberg, P. A., & Démoulin, P. 1998, ApJ, 504, 1006
Lin, J., Soon, W., & Baliunas, S. L. 2003, NewA Rev., 47, 53
Low, B. C. 1984, ApJ, 286, 772
Mikić, Z., & Linker, J. A. 1994, ApJ, 430, 898
Peng, Z., & Hu, Y. Q. 2005, Chinese J. Space Sci., 25, 81
Zhang, Y. Z., Hu, Y. Q., & Wang, J. X. 2005, ApJ, 626, 1096